Journal of Materials Chemistry C

Superior High Temperature Performance of 8 kV NiO/Ga2O3 Vertical Heterojunction Rectifiers

Journal:	*Journal of Materials Chemistry C*
Manuscript ID	TC-ART-04-2023-001200.R1
Article Type:	Paper
Date Submitted by the Author:	03-May-2023
Complete List of Authors:	Li, Jian-Sian; University of Florida, Chemical Engineering Chiang, Chao-Ching; University of Florida, Department of Chemical Engineering Xia, Xinyi; University of Florida, Department of Chemical Engineering Wan, Hsiao-Hsuan; University of Florida, Chemical Engineering Ren, Fan; University of Florida, Department of Chemical Engineering Pearton, Stephen; Univ.Florida, MSE

SCHOLARONE™
Manuscripts

ARTICLE

Superior High Temperature Performance of 8 kV NiO/Ga_2O_3 Vertical Heterojunction Rectifiers

Jian-Sian Li,[a] Chao-Ching Chiang,[a] Xinyi Xia,[a] Hsiao-Hsuan Wan,[a] Fan Ren[a] and S.J. Pearton*[a]

Received 00th January 20xx,
Accepted 00th January 20xx

DOI: 10.1039/x0xx00000x

NiO/β-Ga_2O_3 vertical rectifiers exhibit near-temperature-independent breakdown voltages (V_B) of >8 kV to 600K. For 100 µm diameter devices, the power figure of merit $(V_B)^2$/ R_{ON}, where R_{ON} is the on-state resistance, was 9.1 GW.cm^{-2} at 300K and 3.9 GW.cm^{-2} at 600K. By sharp contrast, Schottky rectifiers fabricated on the same wafers show V_B of ~1100V at 300K, with a negative temperature coefficient of breakdown of 2V/K. The corresponding figures of merit for Schottky rectifiers were 0.22 GW.cm^{-2} at 300K and 0.59 MW.cm^{-2} at 600K. The on-off ratio remained >10^{10} up to 600K for heterojunction rectifiers but was 3 orders of magnitude lower over the entire temperature range for Schottky rectifiers. The power figure of merit is higher by a factor of approximately 6 than the 1-D unipolar limit of SiC. The reverse recovery times were ~26 ±2 ns for both types of devices and was independent of temperature. We also fabricated large area, 1mm^2 rectifiers. These exhibited V_B of 4 kV at 300K and 3.6 kV at 600K. The results show the promise of using this transparent oxide heterojunction for high temperature, high voltage applications.bstract text goes here.

Introduction

The ultra-wide bandgap semiconductors with bandgaps > 3.4 eV include diamond, AlN and Ga_2O_3 and have the potential for significantly higher voltage operation with lower switching losses than commercially available SiC and GaN power devices. The various polytypes of Ga_2O_3 are attracting attention for their potential application in power switching, solar-blind UV detectors and lateral transistors with enhanced two-dimensional electron gases densities [1-7,8]. It is relatively easy to grow bulk crystals of the stable monoclinic β-polymorph from the melt, which enables large-diameter, high-quality substrates for homoepitaxy at potentially low cost [2]. This is attractive for lower manufacturing costs since the material comprises a significant component of the cost of manufacture.

Ga_2O_3 has a high critical electric field strength, which allows for higher operating voltages and lower switching losses in power electronics [1-6]. Its ultrawide bandgap also makes it promising for high temperatures and radiation environment applications. As a result of these advantages, Ga_2O_3 is being considered for several power electronics applications, including inverters, motor drives, and power supplies. There is particular interest in kV-class vertical rectifiers for use in electric vehicles and their charging infrastructure, as well as power management systems for improved switching efficiency for next generation power grids and efficiently interfacing renewable energy sources with these grids [1,4,5]. One of the goals is to achieve a high breakdown voltage and low on resistance, which is a benefit for rectifiers because of lower switching losses. A figure of merit for power electronic devices is defined as $(V_B)^2/R_{ON}$ where V_B is the reverse breakdown voltage and R_{ON-} is the on-state resistance [1,3,4]. To achieve a high-power figure of merit, a rectifier must have a low drift layer concentration, with high electron mobility, as well as low R_{ON}, and optimized edge termination to prevent current crowding [1, 5-21)]. The breakdown voltage is larger for thicker drift layers, but this degrades on-resistance. In addition, vertical geometry devices are desirable, because of their higher power conversion efficiency and absolute currents compared to lateral devices [1,3,4,5]. Power rectifiers are also building blocks for many advanced power handling systems.

The lack of a practical p-type doping capability for Ga_2O_3 has led to integration with p-type oxides to form p-n heterojunctions with the n-type Ga_2O_3 [9-16]. The most successful of these has been NiO, generally deposited by sputtering. The forward current transport mechanism in such junctions is typically recombination at low biases and trap-assisted tunneling at higher bias [10, 21-26]. Promising rectifier performance has been reported with this approach [14-36], including V_B of 8.32 kV, with figure of merit 13.2 GW.cm^{-2} [15].

A less studied aspect has been the elevated temperature performance of such devices [37-42]. In this paper we report an investigation of the temperature dependence of the performance of NiO/Ga_2O_3 and also co-fabricated Au/Ni/Ga_2O_3 vertical rectifiers on the same wafers. While the breakdown voltage of the latter fall-off quickly with increasing temperature, the heterojunction rectifiers exhibit nearly temperature-

[a.] Department of Chemical Engineering, University of Florida, Gainesville, FL 32606 USA.
[b.] Department of Materials Science and Engineering, University of Florida, Gainesville, FL 32606 USA.

† Footnotes relating to the title and/or authors should appear here.
Electronic Supplementary Information (ESI) available: [details of any supplementary information available should be included here]. See DOI: 10.1039/x0xx00000x

independent V_B to 600K. While we focused on small area devices (100μ), we also fabricated large area (1 mm^2) to examine the scaling properties.

Experimental

We made both vertical geometry Schottky rectifiers and NiO/ Ga_2O_3 rectifiers on the same wafers. The bilayer NiO thickness of 10 /10 nm and the length of the NiO extension beyond the top contact (12 µm) to form field plate-like overhang was held constant [17]. The drift region thickness was 10 µm and these layers were grown by halide vapor phase epitaxy (HVPE) on a (001) Sn-doped (10^{19} cm^{-3}) β-Ga_2O_3 single crystal substrate. The samples were purchased from Novel Crystal Technology, Japan. A schematic of the two device structures is shown in Figure 1 (top).

Ohmic contacts were made to the back of the doped substrates using a Ti/Au deposited by e-beam evaporation and annealed at 550 C for 180s under N_2. The front surface was cleaned by UV/Ozone exposure for 15 mins to remove contamination [17]. The 10/10 nm NiO bilayer was deposited after the Ohmic contacts by rf (13.56 MHz) magnetron sputtering at a working pressure of 3mTorr. The hole concentration in these films was adjusted using the Ar/O_2 ratio. The structure was then annealed at 300°C under O_2. Finally, a top contact of 20/80 nm Ni/Au (100 µm or 1mm diameter) was deposited onto the NiO layer and also formed the Schottky contact on those devices. The NiO was extended 12 um beyond the contact metal to form a field-plate-like overhang. C^{-2}-V plots for the drift layer doping showed the carrier concentration was 6.7x10^{15} cm^{-3}. The device design for NiO thickness and extension were guided by TCAD simulations [17].

The current density-voltage (J-V) characteristics were measured on Tektronix 370-A and 371-B curve tracers and Agilent 4156C parameter analyser. For the reverse voltages >2kV, a Glassman power supply was employed and all the measurements were performed in Fluorinert atmosphere to avoid breakdown of the air at these high voltages. The reverse breakdown voltage was defined as the bias for a reverse current reaching 0.1 $A.cm^2$. The devices did not suffer permanent damage at this condition, with identical I-V characteristics as before measurement, but increasing the voltage a further 50-200 V led to permanent failure through breakdown at the NiO/Ga_2O_3 contact periphery. The on-resistance values were calculated assuming the current spreading length is 10 um and a 45° spreading angle. We also subtracted the resistance of the cable, probe and chuck, which was around 10 Ohm.

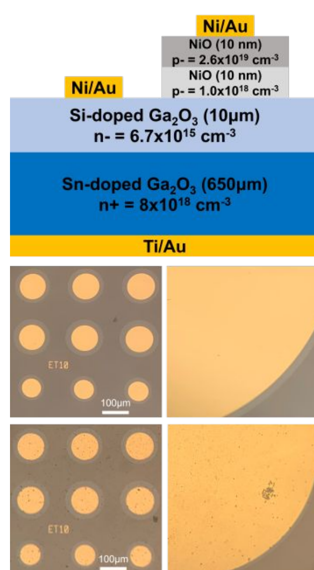

Figure 1. (top) Schematic of structures and images of devices (center) before and (bottom) after operation at 600K.

Results and Discussion

Figure 2 shows the forward J-V characteristics and associated on-state resistances from (a) Schottky (SBD) rectifiers and (b) heterojunction (HJD) rectifiers of 100 µm diameter as a function of temperature. The on-resistance was obtained from the slope of the forward I-V characteristics. The turn-on voltages decrease with increasing temperature in both types of devices, while R_{ON} increases due to the decreased carrier mobility at higher temperatures [4-6]. A Richardson plot for the Schottky rectifiers showed a $e\Phi_{b0}$ value of 0.6 eV and a Richardson's

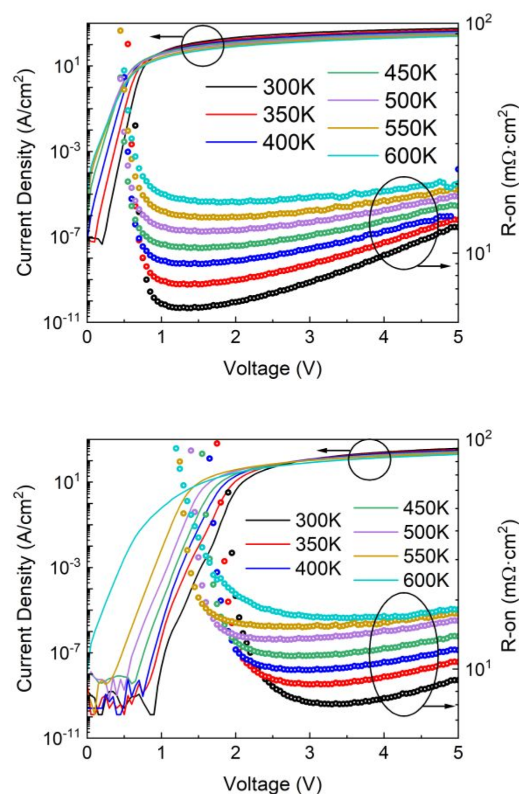

Figure 2. Forward current densities and R_{ON} values for (a) Schottky rectifiers or (b) NiO/Ga_2O_3 as a function of temperature.

 This journal is © The Royal Society of Chemistry 20xx

Please do not adjust margins

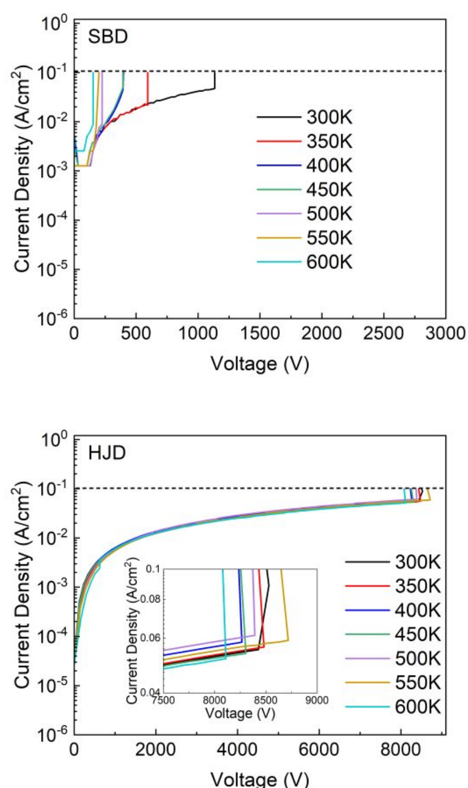

Figure 3. (top). Reverse current characteristics from (a) Schottky rectifier and (bottom) NiO/Ga_2O_3 heterojunction rectifiers as a function of temperature.

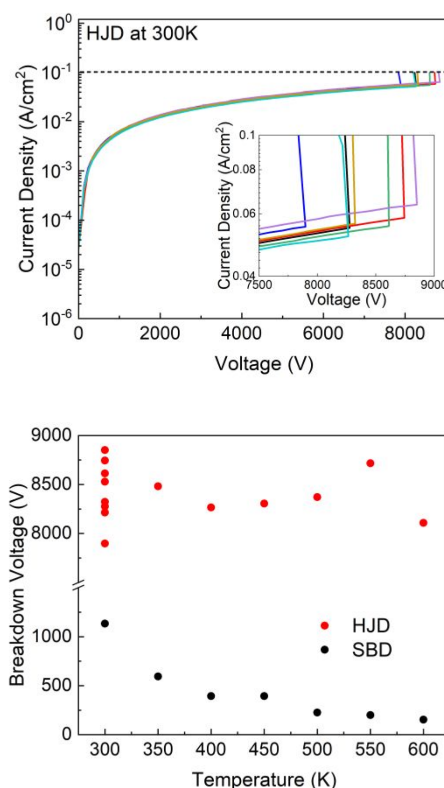

Figure 4. (top) Spread of reverse current characteristics from NiO/Ga_2O_3 heterojunction rectifiers at 300K. (bottom)Temperature dependence of breakdown voltage for Schottky barrier diodes and heterojunction diodes.

constant of 40 A.cm ^{2}. K^{-1}. The barrier height monotonically decreased from 1.02 eV at 300K to 0.65eV at 600K. The R_{ON} values are slightly higher for the HJD, as expected (14-17). Both types can conduct >100 A.cm^{-2} at 4V. Note that the R_{ON} in the heterojunction rectifiers does not continue to decrease at forward voltages beyond ~3V. It has also been shown the band alignment remains type II, staggered gap with the magnitude of the conduction and valence band offsets increasing monotonically with annealing temperature (12).

Figure 3 shows the reverse J-V characteristics for both types of devices at different temperatures. The Schottky rectifiers show a sharp reduction in the breakdown voltage as temperature increases, as shown in Figure 3 (a). By sharp contrast, the heterojunction rectifiers show very little change in breakdown voltage, as shown in Figure 3 (b). Note also that the Schottky devices have breakdown voltages of only ~1100V at 300K, whereas the NiO/Ga_2O_3 devices remain above 8kV across the temperature range up to 600K. This is a remarkable demonstration of the utility of the NiO in forming a robust p-n junction with the Ga_2O_3 and also in providing effective edge termination to mitigate breakdown at the contact periphery. The devices did not show any visible damage after measurement at 600K, as shown in the center and bottom of Figure 1 for the Schottky and heterojunction rectifiers, respectively.

To give an example of the uniformity of the results, Figure 4 (top) shows the spread of reverse current characteristics from eight different NiO/Ga_2O_3 heterojunction rectifiers at 300K. This was from 7.9-8.7 kV, measured over an area of approximately 1cm^2. The trends in V_B with temperature are shown in Figure 4 (bottom) for the two device types, with the same number of Schottky diodes measured. While the

This journal is © The Royal Society of Chemistry 20xx

Please do not adjust margins

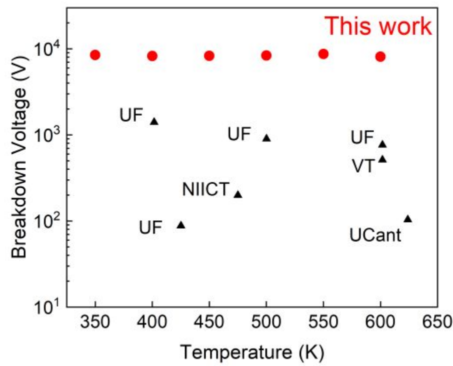

Figure 5. Compilation of maximum operation temperature versus V_B for vertical Ga_2O_3 rectifiers. Previous data comes from Virginia Tech [37], University of Canterbury [39], University of Florida [38] and NIICT [40].

heterojunction devices show no significant change in V_B up to 600K, the Schottky rectifiers show the commonly reported negative temperature coefficient. The temperature dependence of V_B follows an approximate relationship of the form [4, 37-42]:

$$V_B = V_{B0}\left[1 + \beta(T - T_0)\right]$$

where β=–2±0.6 V.K^{-1}. The negative temperature coefficient precludes impact ionization as the breakdown mechanism in the Schottky rectifiers. This is not unexpected, as new materials technologies generally show breakdowns dominated by defect-assisted processes until the materials growth matures. This was the case for GaN, for example [43]. Previous work has shown in vertical geometry Ga_2O_3 rectifiers that impact ionization of deep acceptors is a strong contributor to breakdown [44]. A low or negative temperature coefficient of breakdown does have advantages in preventing the rectifiers from being damaged by excessive voltage. A positive temperature coefficient of breakdown can lead to overvoltage conditions and device failure at high temperatures.

Figure 5 shows a compilation of reported maximum operation temperature versus V_B for vertical Ga_2O_3 rectifiers. There is a clear improvement in the present work, which we ascribe to the advances in crystal growth in lowering the drift layer carrier concentration and extended defect density in the starting wafers and also to optimization of the NiO deposition parameters.

The R_{ON} and turn-on voltages from the Schottky and heterojunction rectifiers are shown as a function of temperature in Figure 6. The R_{ON} values are higher for the heterojunctions and increase with temperature, which we ascribe mainly to the degradation in carrier mobility through

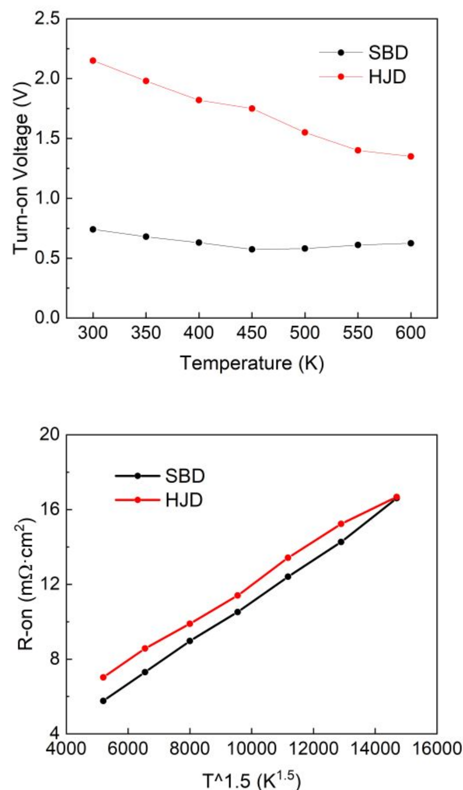

Figure 6. Temperature dependence of on-state resistance and turn-on voltage for Schottky barrier diodes and heterojunction diodes.

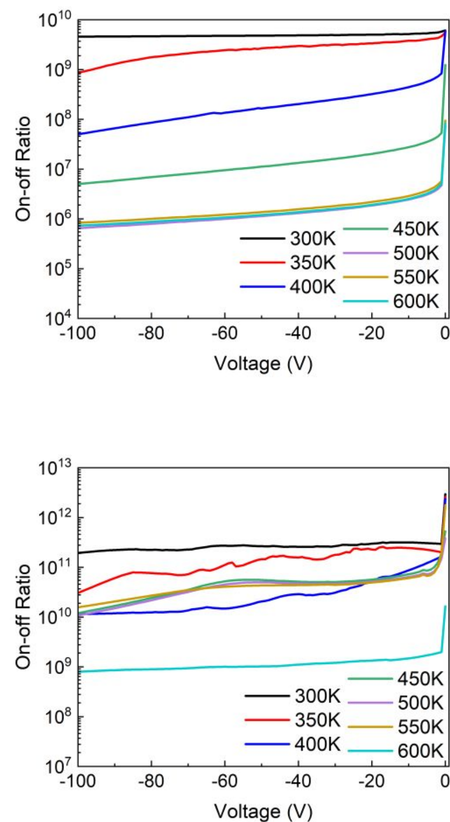

Figure 7. On-off ratio of (top) Schottky rectifiers and (bottom) NiO/Ga_2O_3 heterojunction rectifiers in which the bias was switched from 5V forward to the voltage shown on

This journal is © The Royal Society of Chemistry 20xx

Please do not adjust margins

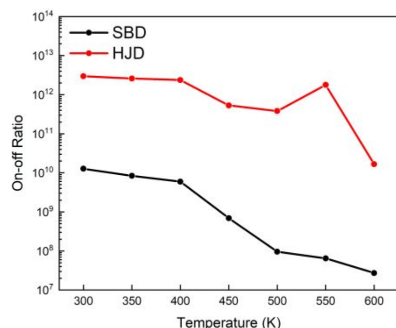

Figure 8. Temperature dependence of on/off ratio for Schottky barrier diodes and heterojunction diodes when switching from 5V forward to 0V.

phonon (lattice) scattering since we could fit the R_{ON} data to a $T^{3/2}$ dependence. Additional evidence could come from extracting mobility from the space charge limited current via the Mott-Gurney Law. The turn-on voltage exhibited a weak dependence on temperature and was lower for the Schottky rectifiers, as expected. The power figure of merits for the heterojunctions were 9.1 GW.cm^{-2} at 300K and 3.9 GW.cm^{-2} at 600K. Note that the theoretical maximum is around 34 MW. cm^{-2}. The corresponding figures of merit for Schottky rectifiers were 0.22 GW.cm^{-2} at 300K and 0.59 MW.cm^{-2} at 600K.

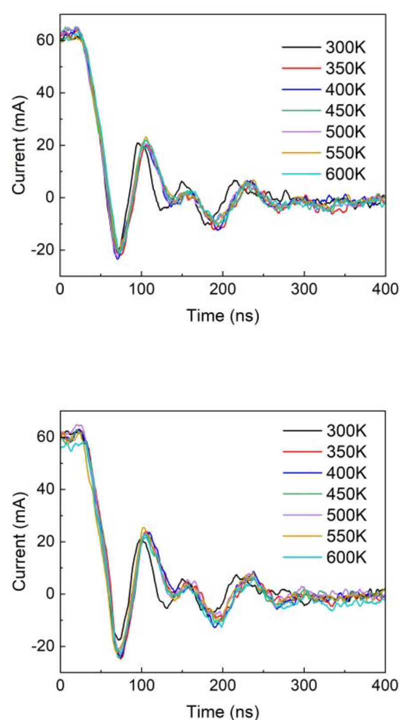

Figure 9. Temperature dependence of switching characteristics of (top) Schottky rectifiers and (bottom) NiO/Ga_2O_3 heterojunction rectifiers in which the devices were switched from 60 mA forward current to zero.

Table 1. Recovery characteristics from Schottky and heterojunction rectifiers.

Temperature (K)	Trr (ns)	Irr (mA)	dI/dT (A/μs)	IF (mA)
Schottky				
300	24	-23	2.7	60
350	28	-26	2.6	60
400	28	-27	2.5	60
450	25	-26	2.3	60
500	27	-25	2.1	60
550	26	-26	2.3	60
600	24	-26	2.2	60
Heterojunction				
300	25	-20	2.4	60
350	25	-27	2.0	60
400	25	-27	2.0	60
450	25	-27	1.9	60
500	23	-26	1.9	60
550	25	-24	1.9	60
600	27	-25	1.9	60

The on-off ratios as a function of temperature when switching from 5V forward bias to the negative voltages shown on the x-axes are shown in Figure 7 for both types of rectifiers. The values are 1-3 orders of magnitude higher for the heterojunctions due to the lower reverse current at a given bias. Even at 600K the on-off ratio is ~10^9 for the NiO/Ga_2O_3 rectifiers.

Figure 8 shows temperature dependence of on/off ratio for (top) Schottky barrier diodes and (bottom) heterojunction diodes for switching from 5 V forward voltage to 0V. These are essentially the maximum on-off ratios achievable in the devices.

The switching characteristics of the rectifiers are also of paramount interest, since they need fast recovery times and the ability to switch large currents [45-63]. Figure 9 shows the temperature dependence of (top) Schottky rectifiers and (bottom) NiO/Ga_2O_3 heterojunction rectifiers of reverse recovery characteristics in which the devices were switched from 60 mA forward current to 0V. The reverse recovery times are ~ 26 ±2 ns and are tabulated in Table 1. The relative indifference to device structure and temperature demonstrates that charge storage in the p-n junction is not a significant factor compared to the Schottky device. We have not seen significant difference in recovery characteristics between small and large devices.

We also examined the temperature dependence of performance of the large area (1 mm^2) heterojunction rectifiers. Figure 10 (top) shows the forward current characteristics. Note that the absolute forward current is >3A for all temperatures, with a breakdown voltage of 4kV at room temperature, as shown in Figure 10 (bottom). The reason for the lower

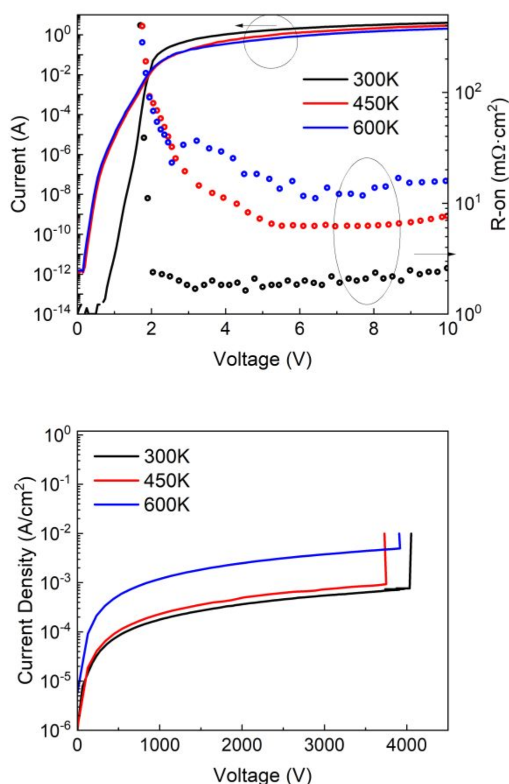

Figure 10. (top) Forward current densities and R_{ON} values and (bottom) reverse current characteristics from 1mm^2 NiO/Ga_2O_3 heterojunction rectifiers as a function of temperature.

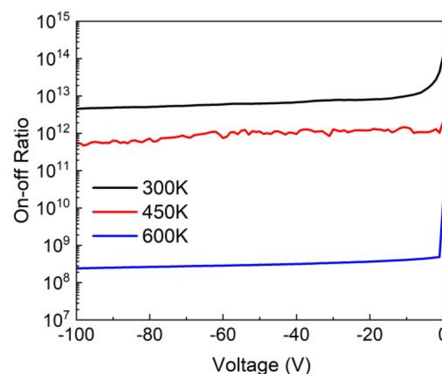

Figure 11. On-off ratio of 1mm^2 NiO/Ga_2O_3 heterojunction rectifiers in which the bias was switched from 10V forward to the voltage shown on the x-axis.

breakdown is not clear and could be due to a higher probability of having intrinsic defects or an issue with field crowding. The power figure-of-merit is 6.4 GW.cm^{-2} at 300K and 0.8 MW.cm^{-2} at 600K. The on-off ratio remained above 10^8 at 600K, for switching to -100V, as shown in Figure 11.

Conclusions

Since the breakdown, forward I-V and on resistance did not degrade to much at 300°C, the concerns of low thermal conductivity of gallium oxide should be of less concern provided the long-term reliability can be established. The power figure of merits reported here are around 26 % of the theoretical maximum for Ga_2O_3 [15]. It is anticipated that continued reduction in defect density, as well as adding other edge termination technology such as field plates, implanted guard rings, mesa etching as possible methods to improve field uniformity can enhance future performance closer to this maximum. This is because bulk Ga_2O_3 crystals are known to have internal planar defects, i.e., plate-like voids and stacking faults, and it is known that higher dislocation densities lead to higher leakage currents in Ga_2O_3 rectifiers [64-66]. This is because the dislocations can act as recombination centers for electrons and holes, leading to an increased probability of carrier recombination and subsequent leakage current and hence lower breakdown voltage.

The NiO/ Ga_2O_3 heterojunction rectifier is potentially an ideal structure for high-voltage and high-power applications, where it can offer better efficiency and reduced energy losses compared to traditional semiconductors. The wide bandgap of both NiO (~3.9 eV) and β-Ga_2O_3 (4.8eV) also makes power rectifiers from this heterojunction attractive for high-temperature applications. These properties make Ga_2O_3 power rectifiers promising for high-power and high-temperature applications such as electric vehicles, power electronics, and aerospace.

Conflicts of interest

There are no conflicts to declare.

Acknowledgements

The work at UF was performed as part of Interaction of Ionizing Radiation with Matter University Research Alliance (IIRM-URA), sponsored by the Department of the Defense, Defense Threat Reduction Agency under award HDTRA1-20-2-0002. The content of the information does not necessarily reflect the position or the policy of the federal government, and no official endorsement should be inferred. The work at UF was also supported by NSF DMR 1856662.

References

1 M. H. Wong and M. Higashiwaki, IEEE T Electron Dev, 2020, 67, 3925.
2 Zbigniew Galazka, J. Appl. Phys .2022, 131, 031103
3 X Lu, Y X Deng, Y L Pei, Z M Chen, and G Wang, Recent advances in NiO/Ga2O3 heterojunctions for power electronics, J. Semicond. (2023, In Press).
4 Andrew J. Green, James Speck, Grace Xing, Peter Moens, Fredrik Allerstam, Krister Gumaelius, Thomas Neyer, Andrea

 This journal is © The Royal Society of Chemistry 20xx

Please do not adjust margins

Arias-Purdue, Vivek Mehrotra, Akito Kuramata, Kohei Sasaki, Shinya Watanabe, Kimiyoshi Koshi, John Blevins, Oliver Bierwagen, Sriram Krishnamoorthy, Kevin Leedy, Aaron R. Arehart, Adam T. Neal, Shin Mou, Steven A. Ringel, Avinash Kumar, Ankit Sharma, Krishnendu Ghosh, Uttam Singisetti, Wenshen Li, Kelson Chabak, Kyle Liddy, Ahmad Islam, Siddharth Rajan, Samuel Graham, Sukwon Choi, Zhe Cheng, and Masataka Higashiwaki, APL Mater.2022, 10, 029201.
5 S. J. Pearton, Fan Ren, Marko Tadjer and Jihyun Kim, J. Appl. Phys., 2018, 124, 220901.
6 Chenlu Wang, Jincheng Zhang, Shengrui Xu, Chunfu Zhang, Qian Feng, Yachao Zhang, Jing Ning, Shenglei Zhao, Hong Zhou and Yue Hao, J. Phys. D: Appl. Phys. 2021, 54, 243001.
7 M. Bosi, P. Mazzolini L. Seravalli and R. Fornari, J. Mater. Chem. C 2020,8, 10975.
8 Kentaro Kaneko, Kazuyuki Uno, Riena Jinno, and Shizuo Fujit , J. Applied Physics 2022, 131, 090902 .
9 Y. Kokubun, S. Kubo and S. Nakagomi, Appl Phys Express,2016, 9, 091101 .
10 Yuxin Deng, Ziqi Yang, Tongling Xu, Huaxing Jiang, Kar Wei Ng, Chao Liao, Danni Su, Yanli Pei, Zimin Chen, Gang Wang, Xing Lu, Appl Surf Sci, 2023, 622, 156917.
11 Maria Isabel Pintor-Monroy, Diego Barrera, Bayron L. Murillo-Borjas, Francisco Javier Ochoa-Estrella, Julia W. P. Hsu, and Manuel A. Quevedo-Lopez, ACS Appl. Mater. Interfaces, 2018, 10, 38159 .
12 Xinyi Xia, Jian-Sian Li, Chao-Ching Chiang, Timothy Jinsoo Yoo, Fan Ren, Honggyu Kim and S. J. Pearton, J. Phys. D: Appl. Phys. 2022, 55, 385105 .
13 Hehe Gong, Xuanhu Chen, Yang Xu, Yanting Chen, Fangfang Ren, Bin Liu, Shulin Gu, Rong Zhang, and Jiandong Ye, IEEE T Electron Dev, 2020, 67, 3341.
14 S. Sharma, K. Zeng, S. Saha, U. Singisetti, IEEE Electron Dev. Lett.2020, 41, 836.
15 Jincheng Zhang, Pengfei Dong, Kui Dang, Yanni Zhang, Qinglong Yan, Hu Xiang, Jie Su, Zhihong Liu, Mengwei Si, Jiacheng Gao, Moufu Kong, Hong Zhou and Yue Hao, Nat Commun 2022, 13, 3900 .
16 Pengfei Dong, Jincheng Zhang, Qinglong Yan, Zhihong Liu, Peijun Ma, Hong Zhou and Yue Hao, IEEE Electron Dev Lett, 2022, 43, 765.
17 Jian-Sian Li, Chao-Ching Chiang, Xinyi Xia, Timothy Jinsoo Yoo, Fan Ren, Honggyu Kim, and S. J. Pearton, Appl. Phys. Lett.2022, 121, 042105 .
18 Y. Lv, Y. Wang, X. Fu, Shaobo Dun, Z. Sun, Hongyu Liu, X. Zhou, X. Song, K. Dang, S. Liang, J. Zhang, H. Zhou, Z. Feng, S. Cai and Yue Hao, IEEE T Power Electr.2021, 36, 6179.
19 C. Liao, Xing Lu, Tongling Xu, Paiwen Fang , Yuxin Deng, Haoxun Luo, Zhisheng Wu, Zimin Chen , Jun Liang, Yanli Pei and Gang Wang, IEEE T Electron Dev, 2022, 69, 5722.
20 Ming Xiao, Boyan Wang, Jingcun Liu, Ruizhe Zhang, Zichen Zhang, Chao Ding, Shengchang Lu, Kohei Sasaki, Guo-Quan Lu, Cyril Buttay and Yuhao Zhang, IEEE T Power Electr 2021, 36, 8565 (2021).
21 X. Lu, Xianda Zhou, Huaxing Jiang, Kar Wei Ng, Zimin Chen, Yanli Pei, Kei May Lau and Gang Wang, IEEE Electr Dev Lett. 2020, .41, 449 .
22 Chenlu Wang, Hehe Gong, Weina Lei, Y. Cai, Z. Hu, Shengrui Xu, Zhihong Liu, Qian Feng, Hong Zhou, Jiandong Ye, Jincheng Zhang, Rong Zhang, and Yue Hao, IEEE Electr Device Lett, 2021, 42, 485.
23 Qinglong Yan, Hehe Gong, Jincheng Zhang, Jiandong Ye, Hong Zhou, Zhihong Liu, Shengrui Xu, Chenlu Wang, Zhuangzhuang Hu, Qian Feng, Jing Ning, Chunfu Zhang, Peijun Ma, Rong Zhang, and Yue Hao, Appl. Phys. Lett. 2021, 118, 122102 .
24 H. H. Gong, X. H. Chen, Y. Xu, F.-F. Ren, S. L. Gu and J. D. Ye, Appl. Phys. Lett., 2020, 117, 022104.
25 Hehe Gong, Feng Zhou, Weizong Xu, Xinxin Yu, Yang Xu, Yi Yang, Fang-fang Ren, Shulin Gu, Youdou Zheng, Rong Zhang, Hai Lu and Jiandong Ye, IEEE T Power Electr., 2021, 36, 12213.
26 H. H. Gong, X. X. Yu, Y. Xu, X. H. Chen, Y. Kuang, Y. J. Lv, Y. Yang, F.-F. Ren, Z. H. Feng, S. L. Gu, Y. D. Zheng, R. Zhang, and J. D. Yue, Appl. Phys. Lett.2021, 118, 202102.
27 W. Hao, Q. He, K. Zhou, G. Xu, W. Xiong, X. Zhou, G. Jian, C. Chen, X. Zhao, and S. Long, Appl. Phys. Lett., 2021, 118, 043501.
28 F. Zhou, Hehe Gong, Weizong Xu, Xinxin Yu, Yang Xu, Yi Yang, Fang-fang Ren, Shulin Gu, Youdou Zheng, Rong Zhang, Jiandong Ye and Hai Lu, IEEE T Power Electr, 2022, 37, 1223 .
29 Qinglong Yan, Hehe Gong, Hong Zhou, Jincheng Zhang, Jiandong Ye, Zhihong Liu, Chenlu Wang, Xuefeng Zheng, Rong Zhang, and Yue Hao, Appl. Phys. Lett. 2022, 120, 092106 .
30 Y. J. Lv, Y. G. Wang, X. C. Fu, S. B. Dun, Z. F. Sun, H. Y. Liu, X. Y. Zhou, X. B. Song, K. Dang, S. X. Liang, J. C. Zhang, H. Zhou, Z. H. Feng, S. J. Cai, and Y. Hao, IEEE T Power Electron. 2021, 36, 6179 .
31 Jiaye Zhang, Shaobo Han, Meiyan Cui, Xiangyu Xu, Weiwei Li, Haiwan Xu, Cai Jin, Meng Gu, Lang Chen and Kelvin H. L. Zhang, ACS Appl. Electron. Mater.2020, 2, 456.
32 Yuangang Wang, Hehe Gong, Yuanjie Lv , Xingchang Fu, Shaobo Dun, Tingting Han, Hongyu Liu, Xingye Zhou, Shixiong Liang, Jiandong Ye, Rong Zhang, Aimin Bu, Shujun Cai and Zhihong Feng, IEEE T Power Electr., 2022, 37, 3743.
33 Jian-Sian Li, Chao-Ching Chiang, Xinyi Xia, Hsiao-Hsuan Wan, Fan Ren and S.J. Pearton, J. Vac. Sci. Technol. A2023, 41, 030401.
34 Zhengpeng Wang, Hehe Gong , Student Member, IEEE, Chenxu Meng, Xinxin Yu , Xinyu Sun, Chongde Zhang, Xiaoli Ji, Fangfang Ren, Shulin Gu, Youdou Zheng, Rong Zhang, and Jiandong Ye, IEEE T Electron Dev, 2022, 69, 981.
35 Boyan Wang, Ming Xiao, Joseph Spencer, Yuan Qin, Kohei Sasaki, Marko J. Tadjer and Yuhao Zhang, IEEE Electr Device Lett. 2023, 44, 221 .
36 F. Zhou, H. H. Gong, Z. P. Wang, W. Z. Xu, X. X. Yu, Y. Yang, F.-F. Ren, S. L. Gu, R. Zhang, Y. D. Zheng, H. Lu, and J. D. Ye , Appl. Phys. Lett. 2021, 119, 262103.
37 Boyan Wang, Ming Xiao, Xiaodong Yan, Hiu Yung Wong, Jiahui Ma, Kohei Sasaki, Han Wang and Yuhao Zhang, Appl. Phys. Lett.,2019, 115, 263503.
38 Xinyi Xia, Minghan Xian, Patrick Carey, Chaker Fares, Fan Ren, Marko Tadjer, S J Pearton, Thieu Quang Tu, Ken Goto and Akito Kuramata, J. Phys. D: Appl. Phys*.* 2021, **54** 305103
39 C. Hou, K.R. York, R.A. Makin, S.M. Durbin, R.M. Gazoni, R.J. Reeves and M.W. Allen, Appl. Phys. Lett. 2020, **117** 203502
40 S. Ahn ,F. Ren , L. Yuan, S.J. Pearton and A. Kuramata, ECS J. Solid State Sci. Technol.2017, **6** P68
41 M. Higashiwaki, K. Konishi, K. Sasaki, K. Goto ,K. Nomura K, Thieu Q T and R. Togashi Appl. Phys. Lett. 2016, **108** 133503
42 W. Hao, Q. He, X. Zhou, X. Zhao, G. Xu and S. Long, "2.6 kV NiO/Ga2O3 Heterojunction Diode with Superior High-Temperature Voltage Blocking Capability," 2022 IEEE 34th International Symposium on Power Semiconductor Devices and ICs (ISPSD), Vancouver, BC, Canada, 2022, pp. 105-108.
43 Lina Cao , Zhongtao Zhu, Galen Harden, Hansheng Ye, Jingshan Wang, Anthony Hoffman and Patrick Fay, IEEE Trans. Electron. Dev.2021, 68, 1228 .
44 E.B. Yakimov, A.Y. Polyakov, I.V. Shchemerov, N.B. Smirnov, A.A. Vasilev, A.I. Kochkova, P.S. Vergeles, E.E. Yakimov, A.V. Chernykh, Minghan Xian, F. Ren, S.J. Pearton, Journal of Alloys and Compounds, 2021, 879,160394,
45 Weibing Hao, Feihong Wu, Wenshen Li, Guangwei Xu, Xuan Xie, Kai Zhou, Wei Guo, Xuanze Zhou, Qiming He, Xiaolong Zhao, Shu Yang and Shibing Long, "High-Performance Vertical β-Ga2O3 Schottky Barrier Diodes Featuring P-NiO JTE with

Please do not adjust margins

Adjustable Conductivity," 2022 International Electron Devices Meeting (IEDM), San Francisco, CA, USA, 2022, pp. 9.5.1-9.5.4.
46 X. Zhou, Q. Liu, W. Hao, G. Xu and S. Long, "Normally-off β-Ga_2O_3 Power Heterojunction Field-Effect-Transistor Realized by p-NiO and Recessed-Gate," 2022 IEEE 34th International Symposium on Power Semiconductor Devices and ICs (ISPSD), Vancouver, BC, Canada, 2022, pp. 101-104.
47 Yuan Qin, Zhengpeng Wang, Kohei Sasaki, Jiandong Ye and Yuhao Zhang, Jpn J. Appl Phys 2023, 62, SF0801.
48 H. Gong, F. Zhou, W. Xu, X. Yu, Y. Xu, Y. Yang, F. Ren, S. Gu, Y. Zheng and R. Zhang, IEEE T Power Electr, 2021, 36, 12213 .
49 J. Yang, C. Fares, R. Elhassani, M. Xian, F. Ren, S.J. Pearton, M. Tadjer and A. Kuramata, ECS J Solid State SC, 8,2019, Q3159 .
50 M. Ji, N.R. Taylor, I. Kravchenko, P. Joshi, T. Aytug, L.R. Cao and M.P. Paranthaman, IEEE T Power Electr, 2020, 36, 41.
51 Z. Islam, M. Xian, A. Haque, F. Ren, M. Tadjer and S.J. Pearton, IEEE T. Electron Dev., 2020, .67, 3056 .
52 Rujun Sun, Andrew R. Balog, Haobo Yang, Nasim Alem, Michael A. Scarpulla, IEEE Electron Device L (in press, 2023).
53 M. Xiao, B. Wang, J. Liu, R. Zhang, R. Zhang, C. Ding, S. Lu, K. Sasaki, G.Q. Lu, C. Buttay and Y. Zhang, IEEE T Power Electr 2021, 36, 8565.
54 H. Gong, F. Zhou, X. Yu, W. Xu, F. Ren, S. Gu, , H. Lu, J. Ye. and R. Zhang, IEEE Electr Device Lett.,2022, 43,773.
55 F. Otsuka, H. Miyamoto, A. Takatsuka, S. Kunori, K. Sasaki and A. Kuramata, A., Appl Phys Express, 2021, 15, 016501.
56 W. Hao, F. Wu, W. Li, G. Xu, X. Xie, K. Zhou, W. Guo, X. Zhou, Q. He, X. Zhao and S. Yang, 2022, December. High-Performance Vertical β-Ga_2O_3 Schottky Barrier Diodes Featuring P-NiO JTE with Adjustable Conductivity. In 2022 International Electron Devices Meeting (IEDM) (pp. 9-5). IEEE.
57 Y. Lv, Y. Wang, X. Fu, S. Dun, Z. Sun, H. Liu, X. Zhou, X. Song, K. Dang, S. Liang. and J. Zhang, IEEE T Power Electr, 2020, 3, .6179.
58 J. Wei, Y. Wei, J. Lu, X. Peng, Z. Jiang, K. Yang and X. Luo, 2022, May. Experimental Study on Electrical Characteristics of Large-Size Vertical β-Ga_2O_3 Junction Barrier Schottky Diodes. In 2022 IEEE 34th International Symposium on Power Semiconductor Devices and ICs (ISPSD) (pp. 97-100). IEEE.
59 J. Yang, F. Ren, Y.-T. Chen, Y.-T. Liao, C.-W. Chang, J. Lin, M. J. Tadjer, S. J. Pearton, and A. Kuramata, IEEE J. Electron Dev., 2019, 7, 57 .
60 Jian-Sian Li, Chao-Ching Chiang, Xinyi Xia, Fan Ren and S. J. Pearton, J. Vac Sci Technol A 2022, 40, 063407.
61 F. Zhou, H.H. Gong, Z.P. Wang, W.Z. Xu, X.X. Yu, Y.Yang, F.F. Ren, S.L. Gu, R. Zhang, Y.D. Zheng and H. Lu, Appl Phys Lett, 2021, 119, 262103.
62 F. Zhou, H. Gong, W. Xu, X. Yu, Y. Xu, Y. Yang, F.F. Ren, S. Gu, Y. Zheng, R. Zhang, and J. Ye, J., IEEE T Power Electr, 2021, 37,1223.
63 J.S. Li, C.C. Chiang, X. Xia, C.T. Tsai, F. Ren, Y.T. Liao and S.J. Pearton, ECS J Solid State SC,2022, 11.105003.
64 Sayleap Sdoeung, Kohei Sasaki, Katsumi Kawasaki, Jun Hirabayashi, Akito Kuramata and Makoto Kasu, Jpn. J Appl Phys., 2023, 62, SF1001 .
65 B. Wang, Ming Xiao, Jack Knoll, Cyril Buttay, Kohei Sasaki, Christina Dimarino and Yuhao Zhang, IEEE Electron Device Lett,2021, 42, 1132.
66 Kenichi Ogawa, Naoya Ogawa, Ryo Kosaka, Toshiyuki Isshiki, Yongzhao Yao and Yukari Ishikawa, J. Electron. Mater.2020, 49, 5190 .

This journal is © The Royal Society of Chemistry 20xx

Please do not adjust margins